Korean J. Chem. Eng., 34(6), 1793-1800 (2017)
DOI: 10.1007/s11814-017-0093-2

pISSN: 0256-1115
eISSN: 1975-7220

A new process of acidic hydrolysis of residual chlorosilane liquid for the preparation of silica and hydrochloric acid

Jixiang Cai*, Bing Huang*,†, Qikun Ma, and Wenwen Zhang***

*The Faculty of Environmental Science and Engineering, Kunming University of Science and Technology, Kunming, Yunnan, China
**Kunming Metallurgical Institute New Materials Co., Ltd., Kunming, Yunnan, China
(*Received 2 August 2016 • accepted 1 April 2017*)

Abstract−We propose a novel process for the preparation of silica and concentrated hydrochloric acid using chlorosilane residual liquid originating from the polysilicon production process. The process was designed and optimized after conducting pilot plant tests. The effects of circulating acid concentration, flow rate, chlorosilane residual liquid treatment load and other factors on silica products were studied. The results showed that the circulating acid flowrate can effectively control the formation of gel, and the amount of chlorosilane residual liquid has significant influence on the hydrolysis efficiency and operation of the hydrolysis tower. The prepared silica was characterized using XRD, XRF, FT-IR, SEM, DLS, TG-MS and N_2 adsorption/desorption experiments. The results indicated that silica consisted of amorphous particles, which were spherical, had surface hydroxyl, and showed heterogeneous distribution. The average particle size was 50-80 μm and had high specific surface area (565.049 m^2g^{-1}), large pore volume (0.449 cm^3g^{-1}), and a narrow pore size distribution (3.419 nm). The new technology provides a simple, efficient and environmentally friendly way for treating chlorosilane residual liquid, as well as a cost-effective method for the preparation of silica.

Keywords: Chlorosilane Residual Liquid, Silica, Hydrochloric Acid, Acidic Hydrolysis Process, Polysilicon

INTRODUCTION

Polysilicon has excellent electrical, optical and thermal properties, and is the most important and basic functional material in the semiconductor, electronic information and solar photovoltaic battery industries [1-9]. With the rapid development of semiconductor and photovoltaic industries, the demand for polysilicon has also increased. There are a number of methods to produce polysilicon, such as silane method [10], fluidized bed [11], metal reduction method [12], and metallurgical method [13]. However, the improved Siemens method [14] is one of the more commonly used methods for producing polysilicon. One of the drawbacks of the method is the residual liquid containing chlorosilane, which is mainly composed of silicon tetrachloride ($SiCl_4$), trichlorosilane ($SiHCl_3$), dichlorosilane (SiH_2Cl_2), hexachlorodisilane (Si_2Cl_6), high boiling silicone oil and metal chloride impurities that are introduced by coarse silica powder and catalyst during the polysilicon production process [15-19]. $SiHCl_3$ and $SiCl_4$ are the main components of chlorosilane residual liquid and account for almost 80% or even 90% of the total residual liquid. In addition, hexachlorobenzene (HCDS) has high added value, though its content is very low [20]. Therefore, to improve the utilization rate of silicon, reduce the environmental pollution and the cost of polysilicon production, the study of utilization of chlorosilane residual liquid has attracted more and more attention [21,22].

Various methods, including hydrolysis [23], drying [24], combustion [25], and crystallization [26] have been reported for treating chlorosilane residual liquid. Breneman et al. [27] synthesized silica particles by hydrolyzing chlorosilane residual liquid with lime slurry at 60 °C; however, with this method it is very easy to produce explosive hydrogen gas, which increases the risk of operation. Herman et al. [28] used spray drying technology to recycle silicon tetrachloride from chlorosilane residual liquid; however, the application of the method as a continuous industrial process and high energy consumption still needs research attention. Compared with the hydrolysis method, multi-stage combustion technology [29] is more effective and thorough to deal with the chlorosilane residual liquid. However, this method requires large energy consumption and investment, and causes severe corrosion to the facility. Therefore, it is significant and imperative to develop an economical and effective process to deal with the chlorosilane residual liquid.

In the present study, a new process for preparing silica and by-product hydrochloric acid using hydrolysis of chlorosilane residual liquid has been put forward. The process parameters were optimized through pilot plant tests, and the operating load parameters were determined. To study the properties of silica particles, the production of silica products was characterized using laser particle size analyzer, X-ray diffraction (XRD), X-ray fluorescence (XRF), scanning electron microscopy (SEM), thermal gravimetric - mass spectrometry (TG-MS), Fourier transform infrared spectrum analysis (FT-IR) and N_2 adsorption/desorption experiments.

EXPERIMENTAL

1. Materials

Chlorosilane residual liquid was supplied by a polysilicon pro-

†To whom correspondence should be addressed.
E-mail: 664031600@qq.com

Table 1. Composition of chlorosilane residual liquid

Materials	SiH_2Cl_2	$SiHCl_3$	$SiCl_4$	HCl
Mass fraction	2.13%	4.85%	93.0%	0.02%

ducing company in Yunnan, and its composition is given in Table 1. Industrial hydrochloric acid (HCl, 30%) was purchased from Sichuan Chemical Co. Ltd.. Industrial water was used to prepare solutions for the experiments.

2. Experimental Apparatus

A process flow diagram for treating chlorosilane residual liquid and recovery of silica and HCl is shown in Fig. 1. The hydrolysis tower has a diameter of 0.2 m and height of 5 m, and was designed for producing silica and recycling hydrochloric acid. The chlorosilane residual liquid is fed from the bottom of hydrolysis tower through pipe filter. Nitrogen is used as a carrier gas and passes air-blast atomization nozzle for atomizing the chlorosilane residual liquid in the hydrolysis tower. The gas flow rate is controlled by gas rotor flow meter. After the hydrolysis reaction, the liquid phase mixture is collected in an intermediate collecting tank, whichis was equipped with an agitator, liquid level meter and pressure meter. To to ensure that the whole system is closed, the liquid level of the middle collecting tank must be able to seal the hydrolysis tower. The solid-liquid mixture of silica and hydrochloric acid is separated using a filter. After washing, the filter residue is collected, and dried. The filtrate (hydrochloric acid) is sent to hydrochloric acid storage tank, while the washing liquid (dilute hydrochloric acid) is placed in the washing liquid tank. In hydrochloric acid enrichment stage, hydrochloric acid present in the hydrochloric acid storage tank is used as hydrolysis liquid to continuously cycle until the concentration of hydrochloric acid is higher than 25%. In normal operation, the filtrate (hydrochloric acid concentration higher than 25%) and washing liquid are mixed by static mixer and is sent to the hydrolysis tower using acid pump for cycling hydrolysis liquid.

3. Optimization of Operating Parameters

The hydrolysis of chlorosilane residual liquid and aqueous solution containing hydrochloric acid (HCl, 20%) was carried out in the hydrolysis tower. It is necessary that the whole equipment is leak checked and is flushed with nitrogen before feeding to ensure safety. The operating parameters of the hydrolysis tower (pressure difference and temperature change in tower) were controlled by adjusting the values of residual liquid flow meter (measuring range from 1-10 L/h) and nitrogen flow meter (measuring range from 2-10 m^3/h). These flow parameters were changed after every ten minutes of the process, whereas the corresponding values of pressure, temperature and tail gas compositions were also collected at the same time.

4. Characterization Techniques

Hydrochloric acid concentration was measured by titration. The residue (silica) was dried in an electric drying oven at 105 °C for 5 hours to obtain dry silica powder. The size distribution of particles of silica powder was determined with a laser particle size analyzer (LPS, MS-2000, UK). The crystal structure of particles was recorded using X-ray diffraction (XRD, D2 Advance, Germany) which used Cu Kα radiation (λ=0.15418 nm) in the 2θ range of 5~80°. The impurities of particles were analyzed by X-ray fluorescence (XRF, EDX8300, China). The morphology of particles was characterized by using scanning electron microscopy (SEM, FEI MLA 650, USA). Nitrogen adsorption/desorption isotherms of particles were collected at 77 K using a gas adsorption analyzer (Quantachrome Instrument, Autosorb-IQ, USA). All of the sam-

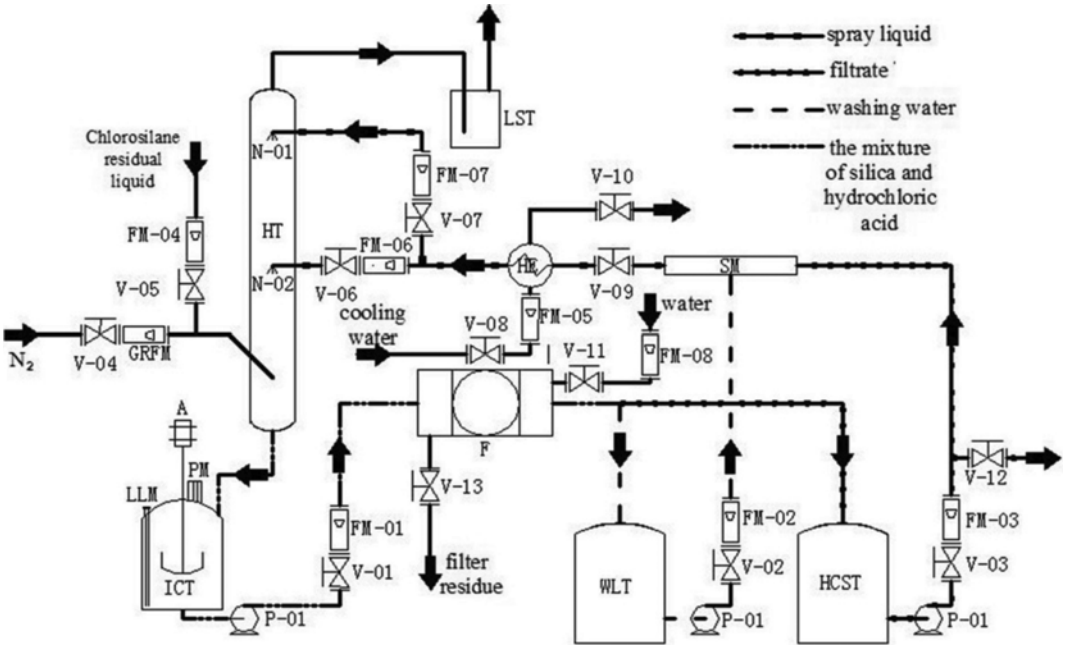

Fig. 1. Process flow diagram. HT-hydrolysis tower; ICT-intermediate collecting tank; LLM-liquid level meter; PM-pressure meter; F-filter; HCST-hydrochloric acid storage tank; WLT-washing liquid tank; SM-static mixer; HE-heat exchanger; LST-liquid seal tank; N-air-blast atomization nozzle; V-valve; P-pump; GRFM-gas rotor flow meter; FM-flow mete.

ples were degassed in vacuum at 90 °C for 1 h and then, at 160 °C for 2 h before analysis. The specific surface area was calculated through Brunauer-Emmett-Teller (BET) method, whereas the total pore volume was calculated from the amount of nitrogen adsorbed at a relative pressure (P/P_0) of 0.99. The average pore size and pore distributions were derived from the desorption branch of N_2 isotherm with Barrett-Joyner-Halenda (BJH) method. Thermal stability, crystal and volatile matter of particles were measured by thermogravimetric-mass spectrometry (TG-MS, thermogravimetric analysis, STA 449 F3 Germany; mass spectrometer, QMS 403 C, Germany). The chemical functional groups of silica were determined by using a Fourier transform infrared (FT-IR) spectrometer (VERTEX70, Germany) with the KBr method.

RESULTS AND DISCUSSION

1. Effect of Circulation Volumes of HCl and Chlorosilane Residual Liquid on the Hydrolysis Reaction

The reaction of chlorosilane residual liquid with hydrochloric acid involved different proportions of circulation volume of HCl and mass of chlorosilane residual liquid. The results are presented in Table 2. Compared to initial concentration, the concentration of hydrochloric acid was increased, but did not reach the theoretically calculated concentration of hydrochloric acid. The hydrolysis reaction was determined to be strongly exothermic. With decrease of circulation volume of HCl, the temperature increased, which accelerated the HCl generated volatilization, resulting in the test concentration of HCl to be lower than the theoretical value. At the same time, the gel phenomenon emerged in the process of hydrolysis reaction, which resulted in an incomplete reaction. Another reason may be that the hydrogen chloride gas produced was not absorbed completely. It is well known that the absorption of hydrogen chloride becomes more difficult at higher concentrations of HCl. The rate of loss of hydrogen chloride also increased with the decrease in circulation volume of HCl, whereas the gelation time decreased (see Table 2). Gel phenomenon will reduce the recovery rate of hydrochloric acid and efficiency of the actual operation. Therefore, it is necessary to control and avoid the gel phenomenon by increasing the circulation volume of HCl, which ensures that the filtration efficiency of particles and the recovery rate of hydrochloric acid are maintained at satisfactory values.

2. Optimization of Process Parameters

2-1. Relationship between Gas Flow in Empty Tower and Pressure Drop

To investigate the relationship between gas flow in empty tower and pressure drop, the pressure drop of the hydrolysis tower was monitored under different nitrogen flow rates while the the amount of circulating spray liquid was maintained at 750 L/h. The experimental results are shown in Fig. 2. With the increase of nitrogen flow rate in the nozzle, the pressure loss increased gradually. This trend was particularly evident when nitrogen flow rate was higher than 7.5 m^3/h. The friction and collisions between the nitrogen and spray droplets in the hydrolysis tower will consume the kinetic energy and correspondingly, increase the resistance of fluid, which will result in the loss of pressure. The collisions will become more intense and pressure loss will gradually increase with the increase in nitrogen flow rate. Therefore, the maximum airflow load of hydrolysis tower is 7.5 m^3/h based on the pilot plant. So, the nitrogen flow rate of nozzle should not be more than 7.5 m^3/h to avoid large pressure drops in the column.

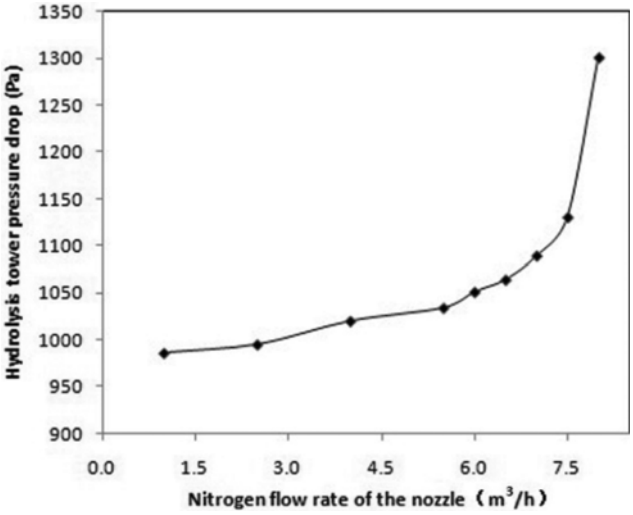

Fig. 2. Relationship between the gas flow rate in empty tower and pressure drop.

2-2. Relationship between Chlorosilane Residual Liquid Flow Rate and Pressure Drop

For the spray liquid and nitrogen flow rates of 750 L/h and 5 m^3/h (or 6 m^3/h), respectively, the pressure drop of the hydrolysis tower was observed by changing the residual liquid flow rate. The experimental results are shown in Fig. 3.

Under nitrogen flow rate of 5 m^3/h or 6 m^3/h, the pressure drop of the hydrolysis tower was not significant with the increase in the residual liquid flow rate (see Fig. 3). However, when the residual liquid flow rate was higher than 9 L/h, the pressure drop increased

Table 2. The results of chlorosilane residual liquid reaction with 20% of hydrochloric acid

No.	The ratio of chlorosilane residual liquid to circulation volume of HCl (kg/m^3)	Theoretical concentration of HCl (%)	Final temperature (°C)	Test concentration of HCl (%)	Loss rate of HCl (%)	Gelation time (min)
1	35.30	22	25	21.2	3.64	360
2	67.34	24	37	23.5	2.08	30
3	100.56	26	42	24.1	7.31	20
4	135.02	28	50	25.1	10.40	17
5	170.80	30	60	24.6	18.00	21

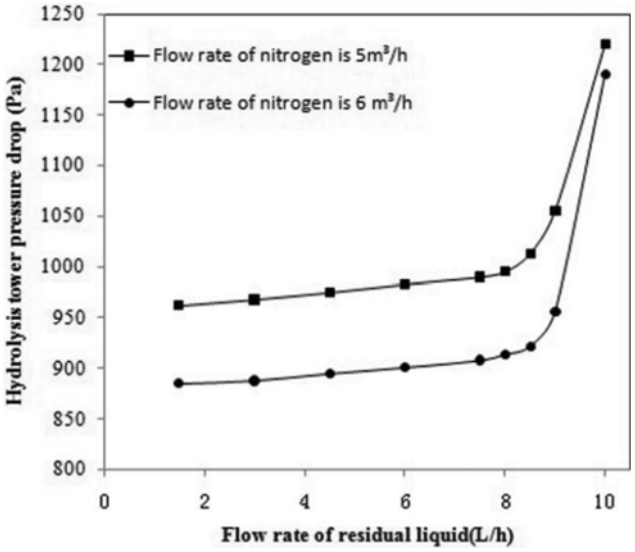

Fig. 3. Relationship between the flow rate of residual liquid and pressure drop.

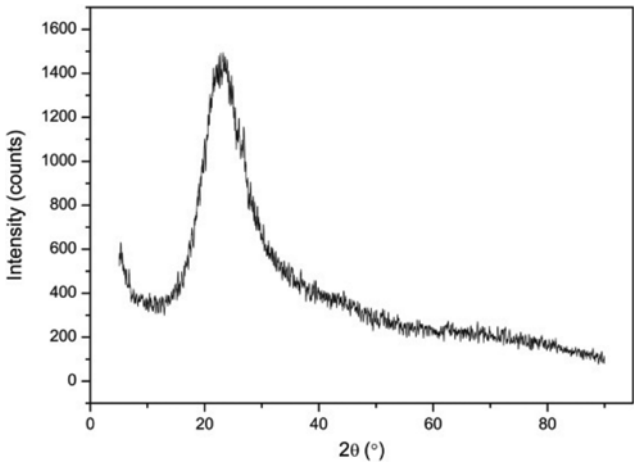

Fig. 4. The XRD pattern of samples.

suddenly. When the residual liquid flowrate was 9 L/h, it would produce around 2.82 m^3/h of hydrogen. The amount of hydrogen produced and the amount of nitrogen (5 m^3/h) exceeded the maximum gas load (7.5 m^3/h) for the tower. Therefore, the pressure drop suddenly increased for chlorosilane residual liquid's flowrate of 9 L/h. The other reason is that the velocity of the gas in the tower reached the fully-turbulent regions, which means that the resistance loss was proportional to the square of the velocity of fluid. This led to a large amount of energy loss. The results showed that the flow rate of the chlorosilane residual liquid (or the maximum processing load of the hydrolysis tower) was less than 9 L/h.

2-3. Effect of Nitrogen Flow Rate on the Hydrolysis Efficiency

When the flowrates of circulating spray liquid and residual liquid were fixed at 750 L/h and 9 L/h (maximum load of the hydrolysis tower), respectively, the tail gas composition was analyzed using the gas chromatography at different nitrogen flow rates. The corresponding results are presented in Table 3.

Chlorosilane was not detected in the exhaust gas (see Table 3), which meant that the chlorosilane residual liquid was completely hydrolyzed. The hydrolysis efficiency in hydrolysis tower can be higher than 99% for nitrogen flowrate of less than 7.5 m^3/h. However, the chlorosilane gas was detected in the tail gas for nitrogen flowrate of more than 7.5 m^3/h. Although the increase in gas velocity can enhance the gas-liquid mass transfer, this also shortens the residence time, which results in incomplete reaction of chlorosilane gas. Moreover, high volatilization of hydrochloric acid was exacerbated due to gas stripping. Therefore, the operation should avoid nitrogen flowrates of higher than 7.5 m^3/h.

3. Characterization of Product Performance

3-1. Phase and Chemical Composition

The X-rap diffraction pattern shown in Fig. 4 confirms that the particles are silica, which have a few other impurities present in them. The wide-angle XRD patterns showed a broad diffraction peak at $2\theta \approx 24.46^{\circ}$, which was the main reflection plane (002) (JSPDS 00-050-1432) of silica. Additionally, no sharp diffraction peak was observed, indicating that the silica produced by hydrolysis method was amorphous [30]. The chemical components of silica particles were analyzed by XRF technique. The results showed that the silica content of samples exceeded 97.57%, and the samples have chlorine content of around 2.21%. In addition, very few impurities were detected, and included 0.0051% Fe, 0.0006% Mn, 0.0004% Cu and other trace elements (Zn, Pb, and Cr). These impurities might have been introduced by the industrial hydrochloric acid. At the same time, due to the adsorptivity of silica, the content of impurities was also enriched during the continuous enriching process of hydrochloric acid.

3-2. Chemical Functional Groups

The obtained particles were confirmed to be silica by FT-IR analysis (as shown in Fig. 5). The absorption bands at 452.22, 763.76 and 1,072.54 cm^{-1} were the rocking vibration, symmetric stretching vibration, and asymmetric stretching vibration of Si-O-Si bond,

Table 3. Composition analysis of off-gas

Flow rate of nitrogen gas in nozzle (m^3/h)	H_2 (%)	O_2 (%)	N_2 (%)	HCL (%)	SiH_2Cl_2 (%)	$SiHCl_3$ (%)	$SiCl_4$ (%)
2.5	0.24	0.35	99.41	<0.01	<0.01	<0.01	<0.01
5.0	0.06	0.08	99.70	<0.01	<0.01	<0.01	<0.01
6.0	0.25	0.14	99.61	<0.01	<0.01	<0.01	<0.01
7.5	0.23	0.24	99.53	<0.01	<0.01	<0.01	<0.01
8.0	0.29	0.17	99.88	0.60	<0.01	0.06	<0.01
9.0	0.27	0.13	99.06	0.50	<0.01	0.04	<0.01

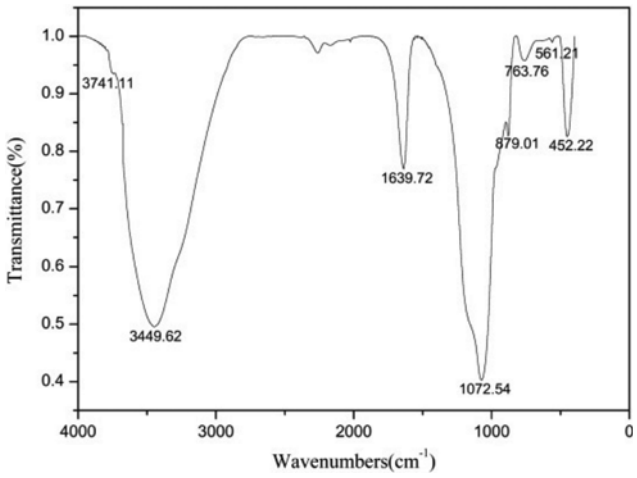

Fig. 5. FT-IR spectra of silica.

respectively, which is similar to the peaks of silica reported in the literature [31]. The band at 561.21 cm^{-1} was linked to a coupled mode in four-member siloxane rings ($[SiO]_4$) [32]. The peak around 1,639.72 cm^{-1} can be ascribed to the bending vibration of H-O-H bond, which indicates the existence of water molecule. The peak at 3,449.62 cm^{-1} belongs to the stretching vibration of H-O-H, indicating the existence of structural water. However, the peak at 879.01 cm^{-1} revealed the bending vibration of Si-OH bond [33-35]. In addition, the weak absorption band at 3,741.11 cm^{-1} was assigned to the stretching vibration of isolated silanols or terminal silanols [36], which were difficult to remove [37]. The presence of these characteristic peaks confirmed the existence of Si-O-Si, Si-OH, and H-O-H bands in the silica particles, which further confirmed that silica can be used to produce fumed silica.

3-3. Morphological Characteristics and Porous Structure

The SEM images of silica under different magnifications are shown in Fig. 6. It is apparent that the silica shape was spherical and had a very poor dispersion. The presence of missing and irregular particles was obvious and meant that inhomogeneous spherical particles were obtained under the conditions as applied in the current work. The size of silica particles was larger during the aggregation of silica. A loose network structure was observed in the silica particles. In addition, flakes of silica were also observed.

The specific surface area of the silica particles was experimentally determined through low temperature nitrogen adsorption-desorption isotherms (see Fig. 7(a)). The shape of the isotherms of the silica particles conformed to Type IV, which is a typical characteristic of mesoporous materials as classified by the International Union of Pure and Applied Chemistry (IUPAC) [38]. Moreover, the adsorption/desorption isotherms were not consistent over a wide range of relative pressure (P/P_0=0.4-0.8). The type of hysteresis loop was IUPAC H3, which was caused by the capillary condensation of nitrogen in mesopores [39]. The corresponding pore size distribution curve of synthetic silica particles is shown in Fig. 7(b). The silica particles exhibited a narrow pore size distribution centered at 3.419 nm, which belonged to a relatively wide mesoporous size distribution range (2-50 nm). On the other hand, the most probable aperture (3.419 nm) was close to the average pore size (3.178 nm), suggesting the uniform porosity of the materials.

3-4. Effect of Circulating HCl Concentration on the Particle Size of Product

The results of concentration of hydrochloric acid and corresponding silica particle size (analyzed by laser particle size analyzer) are presented in Table 4.

The results show that the average particle size of the sample was 50-80 μm, which is not affected by the concentration of circulat-

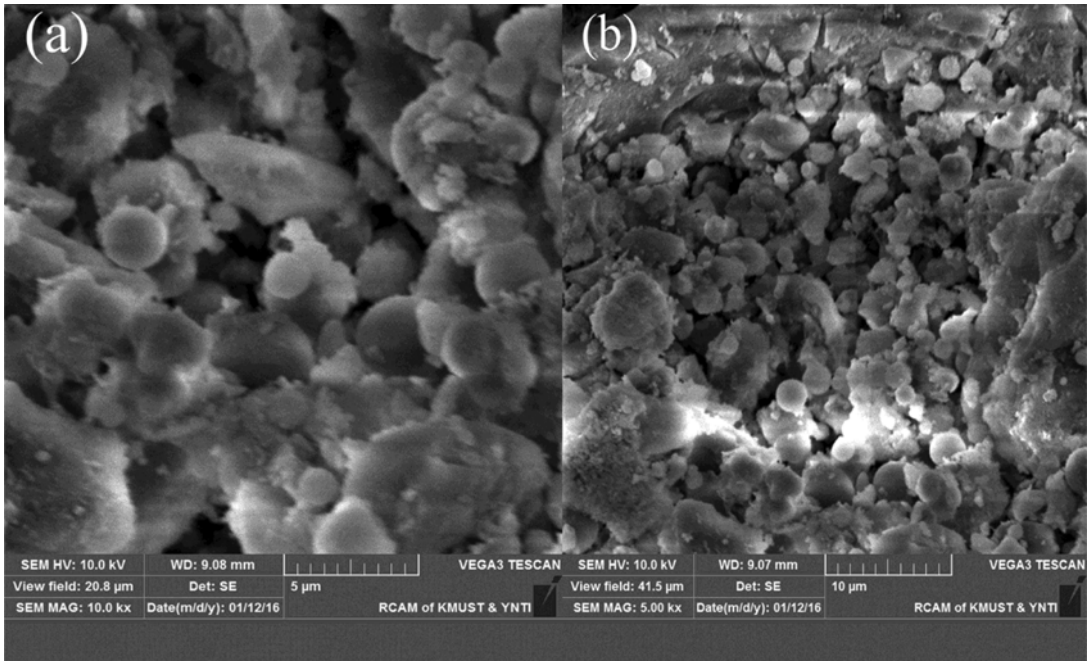

Fig. 6. SEM images of silica at different magnification. (a) ×10000; (b) ×5000.

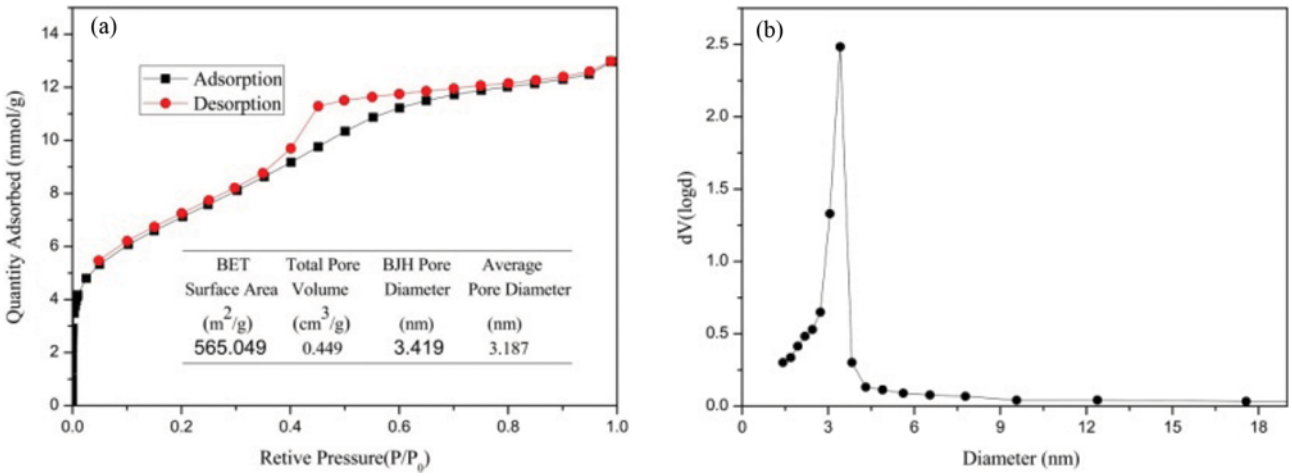

Fig. 7. (a) N_2 adsorption-desorption isotherms and (b) pore size distribution.

Table 4. The particle size of product at different concentrations of hydrochloric acid

No.	1	2	3	4	5	6	7	8	9	10	11	12
Concentration of circulating HCl (%)	1.10	1.57	2.95	5.00	21.23	21.28	21.28	23.20	23.21	24.69	25.90	26.90
Average particle size (μm)	74	63	76	69	72	68	56	61	61	59	60	61

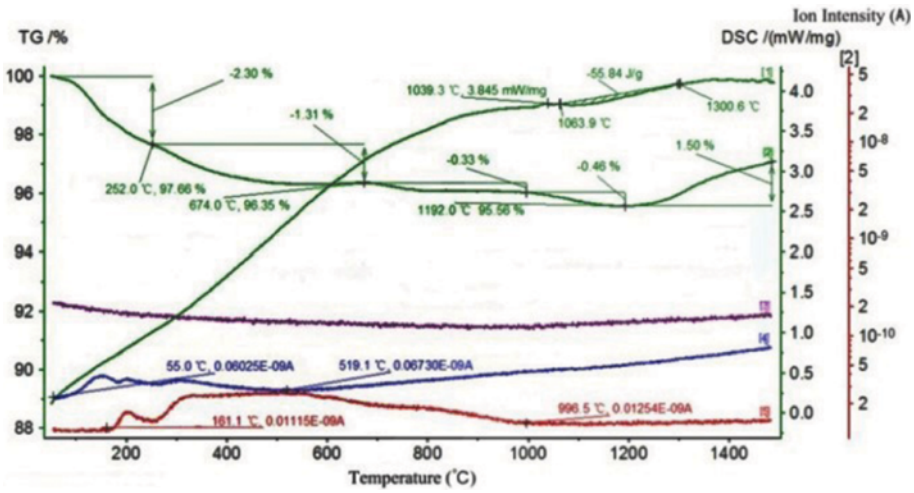

Fig. 8. TG-MS curves of silicas.[1]-Differential thermal curve; [2]-thermogravimetric curves; [3]-HCl; [4]-H_2O; [5]-H_2.

ing hydrochloric acid (see Table 4). By means of infrared spectrum and morphological structure analyses of the product, it was confirmed that the silica particles underwent significant aggregation, which led to large particle size. In the experimental process, due to low efficiency of the filter, the residence time of silica in intermediate collecting tank was too long, which gave silica sufficient time to aggregate. Additionally, it was not filtered on time, which resulted in a higher silica concentration in the intermediate collection tank. The higher concentration of silica will accelerate the nucleation rate of silica and increase the degree of aggregation, eventually leading to an increase in silica particle size. During the operation, it is very important to reduce the residence time of the silica in the hydrolysis system for avoiding particle aggregation and reducing grain diameter of the silica.

3-5. Thermal Stability Analysis of Products

The silica was tested by TG-MS, and the results are shown in Fig. 8. The process of weight loss can be divided into five stages. The first stage occurred at 55-252 °C with the weight loss of 2.30%. Differential thermal curves (DSC) showed that there was slight endothermic reaction peak when the temperature was around 150 °C. From the mass spectra, it is found that the free water and adsorbed water were removed, and a small amount of H_2 was evaporated due to the pyrolysis of Si-H at this temperature. Destruction of bound-water, desorption of adsorbed water on the surface of silica and the pyrolysis of Si-H were overall endothermic, resulting in a small endothermic peak which could be seen in this temperature range. This indicates that silica has a large amount of free water and adsorbed water. Most of the water can easily be removed by

heating. The second stage occurred at a temperature range of 252-674 °C with the weight loss of 1.31%. Mass spectrum (MS) curve showed that due to the dehydration reaction and pyrolysis reaction of Si-H, H_2 and water of crystallization were removed in this stage. The reason for the loss of crystalline water is the emergence of germinal hydroxyl, vicinal hydroxyl and isolated hydroxyl due to dehydration condensation [40,41]. The germinal hydroxyl is defined as two hydroxyl groups appearing on the same silicon atom, while the appearance of two hydroxyl groups appearing on two adjacent silicon atoms is called vicinal hydroxyl [42]. The isolated hydroxyl is only one hydroxyl group on silicon atoms, and there is no hydroxyl group on the adjacent silicon atoms [43]. A large number of hydroxyl groups were removed, which indicated that the reactivity of the silica surface was reduced, hence seriously affecting the application of silica. When the temperature was higher than 674 °C, isolated hydroxyls were slowly dehydroxylated and Si-H bonds were continuously pyrolyzed, until the temperature was close to 996.5 °C, when the crystal water had been completely removed, which in turn indicated that the surface hydroxyl groups of silica had all been removed. At the same time, Si-H bonds were pyrolyzed completely. H_2 release was also complete and the corresponding weight loss in this stage was 0.33%. This means that the isolated hydroxyl and Si-H bonds in the silica are relatively stable, which need to be removed at a higher temperature. When the temperature was 1,039.3 °C, there was a weak endothermic reaction peak, which is due to the phase transformation reaction (silica samples from the solid phase changing to liquid phase). A wide exothermic reaction peak was observed in the temperature range of 1,063.9-1,300.6 °C, for which the peak area was −55.84 J/g. The reason is that the silica samples were converted from amorphous to crystalline structure, whereas the thermal effect of the sample was mainly due to the recrystallization process. These results show that the temperature should not exceed 1,000 °C in the heat treatment process. Higher than 1,000 °C, the silica will undergo a change in the structure of crystal, which will result in complete loss of silica activity.

CONCLUSIONS

A novel process for treating chlorosilane residual liquid has been proposed. The recovery and utilization of chlorosilane residual liquid is resolved by using the acidic hydrolysis of the chlorosilane residual liquid to prepare the silica and by-product concentrated hydrochloric acid. In this process, the hydrolysis efficiency of hydrolysis tower can reach 99% or above and can also successfully enhance the concentration of hydrochloric acid. The silica has amorphous structure with few impurities. It contains surface hydroxyl groups and the distribution is heterogeneous. Moreover, the synthetic silica has a high purity (97.57%), high surface area (565.049 m^2g^{-1}), large pore volume (0.449 cm^3g^{-1}), and narrow pore size distribution (3.419 nm). The silica could lose weight due to the loss of different forms of water and hydroxyls during heating. Under optimized operational parameters of pilot plant (nitrogen flowrate should not be higher than 7.5 m^3/h, the residual liquid flowrate should be less than 9 L/h and circulating spray liquid should be fixed at 750 L/h), the concentration of circulating hydrochloric acid has no significant effect on the product quality (particle size). However, due to the lower circulation flowrate of hydrochloric acid, gel will be formed. The filtration efficiency is low and the residence time of silica in the intermediate collecting tank is too long, due to which the agglomeration of particles is aggravated, leading to increased silica particle size. The average particle diameter of measured samples is 50-80 μm. The process for preparation of silica and concentrated hydrochloric acid by acidic hydrolysis of chlorosilane residual liquid provides a simple, efficient and environmentally friendly method, which is significant for promoting sustainable development of the polysilicon industry.

ACKNOWLEDGEMENT

This study was financially supported by the National Nature Science Foundation of China (grant No. 41261079) and Kunming Metallurgical Institute New Materials Co., Ltd.

REFERENCES

1. A. P. Alivisatos, *J. Phys. Chem.*, **100**, 13226 (1996).
2. W. W. Yu, J. C. Falkner, B. S. Shih and V. L. Colvin, *Chem. Mater.*, **16**, 3318 (2004).
3. M. Su, *Korean J. Chem. Eng.*, **34**, 484 (2017).
4. E. Pihan, A. Slaoui, P. R. I. Cabarrocas and A. Focsa, *Thin Solid Films*, **451**, 328 (2004).
5. Y. Ding, R. Yamada, R. Gresback, S. Zhou, X. D. Pi and T. Nozaki, *J. Phys. D: Appl. Phys.*, **47**, 9 (2014).
6. O. Yasar-Inceoglu, T. Lopez, E. Farshihagro and L. Mangolini, *Nanotechnology*, **23**, 10 (2012).
7. J. Zhang, S. Chen, H. Zhang, S. Zhang, X. Yao and Z. Shi, *RSC Adv.*, **6**, 12061 (2016).
8. C. M. Carbonaro, R. Corpino, P. C. Ricci, M. Salis and A. Anedda, *J. Mater. Sci.*, **48**, 4452 (2013).
9. C. Chen, K. S. You, J. W. Ahn and W. S. Ahn, *Korean J. Chem. Eng.*, **27**, 1010 (2010).
10. B. G. Gribov and K. V. Zinov'ev, *Inorg. Mater.*, **39**, 653 (2003).
11. X. Z. Chen, D. P. Shi, X. Gao and Z. H. Luo, *Powder Technol.*, **205**, 276 (2011).
12. E. Robert and T. Zijlema, US Patent, 7,943,109 (2011).
13. A. F. B. Braga, S. P. Moreira, P. R. Zampieri, J. M. G. Bacchin and P. R. Mei, *Sol. Energy Mater. Sol. Cells*, **92**, 418 (2008).
14. D. Lynch, *Jom*, **61**, 41 (2009).
15. S. Kirii, M. Narukawa and H. Takesue, US Patent, 6,846,473 (2005).
16. N. Masuda and N. Tachino, US Patent, 8,197,783 (2012).
17. W. C. Breneman, EP Patent, 1622831 A1 (2006).
18. L. Fabry, U. Paetzold and M. Stepp, US Patent, 8,557,210 (2013).
19. K. Hesse and F. Schreieder, US Patent, 7708970 B2 (2010).
20. K. Naumann, G. Zon and K. Mislow, *J. Am. Chem. Soc.*, **91**, 7012 (2002).
21. W. M. Nelson, P. Naidoo and D. Ramjugernath, *J. Chem. Thermodyn.*, **91**, 420 (2015).
22. G. Szabo, D. Szieberth and L. Nyulaszi, *Struct. Chem.*, **26**, 231 (2015).
23. K. Ruff, US Patent, 5,080,804 (1992).
24. R. A. Burgie and O. A. Heng, US Patent, 5,118,486 (1992).

25. S. Ferron, J. Kelly and R. Vermeulen, US Patent, 7569193 B2 (2009).
26. L. Stephen Michael, US Patent, 7,736,614 (2010).
27. W. C. Breneman and D. M. Reeser, US Patent, 4,690,810 (1987).
28. J. E. Herman, US Patent, 6,090,360 (2000).
29. L. M. Coleman and W. Tambo, US Patent, 4519999 A (1985).
30. X. L. Zhang and Y. L. Fan, *J. Non-Cryst. Solids*., **358**, 337 (2012).
31. P. R. Pinto, L. C. Mendes, M. L. Dias and C. Azuma, *Colloid. Polym. Sci*., **284**, 529 (2006).
32. A. Fidalgo, R. Ciriminna, L. M. Ilharco and M. Pagliaro, *Chem. Mater*., **17**, 6686 (2005).
33. N. Pijarn, A. Jaroenworaluck, W. Sunsaneeyametha and R. Stevens, *Powder Technol*., **203**, 462 (2010).
34. T. Uchino, A. Aboshi, S. Kohara, Y. Ohishi, M. Sakashita and K. Aoki, *Phys. Rev. B*., **69**, (2004).
35. S. Lee and R. Ha, *Korean J. Chem. Eng*., **33**, 2469 (2016).
36. F. Yan, J. G. Jiang, S. C. Tian, Z. W. Liu, J. Shi, K. M. Li, X. J. Chen and Y. W. Xu, *Acs Sustain. Chem. Eng*., **4**, 4654 (2016).
37. S. Cerveny, G. A. Schwartz, J. Otegui, J. Colmenero, J. Loichen and S. Westermann, *J. Phys. Chem. C*., **116**, 24340 (2012).
38. M. Su, H. J. Su, B. L. Du, X. T. Li, G. Y. Ren and S. D. Wang, *Korean J. Chem. Eng*., **32**, 852 (2015).
39. F. Adam, K. Kandasamy and S. Balakrishnan, *J. Colloid Interface Sci*., **304**, 137 (2006).
40. J. M. Kim, S. M. Chang, S. M. Kong, K. S. Kim, J. Kim and W. S. Kim, *Ceram. Int*., **35**, 1015 (2009).
41. S. Ek, A. Root, M. Peussa and L. Niinisto, *Thermochim. Acta*, **379**, 201 (2001).
42. X. J. Chen, J. G. Jiang, F. Yan, S. C. Tian and K. M. Li, *RSC Adv*., **4**, 8703 (2014).
43. P. K. Jal, M. Sudarshan, A. Saha, S. Patel and B. K. Mishra, *Colloids Surf., A*, **240**, 173 (2004).